fractal and fractional

MDPI

Article

The Impact of Sentinel-1-Corrected Fractal Roughness on Soil Moisture Retrievals

Ju Hyoung Lee [1,*] and Hyun-Cheol Kim [2]

[1] Department of Geography, Environment and Geomatics, University of Guelph, 50 Stone Rd E, Guelph, ON N1G 2W1, Canada
[2] Center of RS & GIS, KOPRI 26, Songdomirae-ro, Yeonsu-gu, Incheon 21990, Republic of Korea
* Correspondence: lee06@uoguelph.ca

Abstract: Fractals are widely recognized as one of the best geometric models to depict soil roughness on various scales from tillage to micro-topography smaller than radar wavelength. However, most fractal approaches require an additional geometric description of experimental sites to be analysed by existing radiative transfer models. For example, fractal dimension or spectral parameter is often related to root-mean-square (RMS) height to be characterized as the microwave surface. However, field measurements hardly represent multi-scale roughness. In this study, we rescaled Power Spectral Density with Synthetic Aperture Radar (SAR)-inverted rms height, and estimated non-stationary fractal roughness to accommodate multi-scale roughness into a radiative transfer model structure. As a result, soil moisture was retrieved over the Yanco site in Australia. Local validation shows that the Integral Equation Model (IEM) poorly simulated backscatters using inverted roughness as compared to fractal roughness even in anisotropic conditions. This is considered due to a violation of time-invariance assumption used for inversion. Spatial analysis also shows that multi-scale fractal roughness better illustrated the hydrologically reasonable backscattering partitioning, as compared to inverted roughness. Fractal roughness showed a greater contribution of roughness to backscattering in dry conditions. Differences between IEM backscattering and measurement were lower, even when the isotropic assumption of the fractal model was violated. In wet conditions, the contribution of soil moisture to backscattering was shown more clearly by fractal roughness. These results suggest that the multi-scale fractal roughness can be better adapted to the IEM even in anisotropic conditions than the inversion to assume time-invariance of roughness.

Keywords: soil roughness; soil moisture; fractal method; power-law spectrum; synthetic aperture radar (SAR)

Citation: Lee, J.H.; Kim, H.-C. The Impact of Sentinel-1-Corrected Fractal Roughness on Soil Moisture Retrievals. *Fractal Fract.* **2024**, *8*, 137. https://doi.org/10.3390/fractalfract8030137

Academic Editor: Mihai Ivanovici

Received: 10 October 2023
Revised: 30 January 2024
Accepted: 21 February 2024
Published: 27 February 2024

1. Introduction

Radars remotely sense the microwave signals of natural surfaces to provide us with high-resolution geological and geographical features. In dry soils devoid of vegetation, the signals of synthetic aperture radar (SAR) are mainly attributed to the morphological properties of the land surface. On Earth, SAR imagery is applied to investigate geological features in the volcanic and desert regions [1]. Thus, radar backscattering amplitude is often used to explore natural surfaces not only on the Earth but also on other planets in this solar system [1]. For example, the land surface of the moon is observed with miniature synthetic aperture radar (Mini-SAR) at S- or X-band [2]. It is used to investigate several issues such as human outposts and rover trafficability. In addition to geography, SAR images are also employed to monitor various disasters such as flooding, landslides, oil spills, or forest fires. For example, Di Martino, et al. [2] suggested fractal geometry to monitor inundated areas with SAR images. Voigt, et al. [3] applied SAR images to assess the landslide-affected area in the Philippines.

In particular, SAR-retrieved roughness is widely used for various applications. Geologically, a change in surface roughness in volcanic areas reveals eruption patterns, lava

age, or the distribution of lava flow [4]. It is also useful to monitor alluvial depositions in arid areas, as they are related to climate change-driven surface instability [5]. In this study, SAR roughness is referred to as a geometric and topographic feature of the natural surface factors that alter SAR backscatter on multi-scales from several millimetres to several meters: the small scale is affected by speckle or micro-topography such as a type of grain at the scale of radar wavelength; the intermediate scale is affected by vegetation at sub-pixel levels; the large scale is related to overall image texture due to incidence angle, orientation, tillage, or mountain [2,6]. The effect of roughness on SAR backscatter affects the retrievals of soil moisture because radar backscattering is sensitive to both dielectric (soil moisture) and geometric (roughness) soil surface properties [7]. If other parameters such as sensor configuration and roughness are fully determined, dielectric constants are all that remains to infer soil moisture from SAR backscattering. Thus, the appropriate estimation of roughness is an important prerequisite for successful soil moisture retrievals.

In general, the roughness locally measured in the field is expressed as a vertical (root-mean-square, [8] rms height) or horizontal (correlation length) variation [9]. This intrinsic roughness is on the small scales near the radar wavelength approximately 5cm for the C-band. If the surface is 'stationary' random with a Gaussian height distribution, a mean elevation, and a standard deviation of surface height, an autocorrelation function (ACF) can provide a statistical description of the surface as constants. They can be directly measured in the field with a mesh board profiler, laser profilometer, laser scanner, pin profiler, needle, or 3D photogrammetry [10,11]. However, it takes too much effort and time to acquire a high density of measurements to construct a variability in surface micro-topography. In addition, it is common to measure a transect of surface roughness in an isotropic condition. However, SAR data are not isotropic as usual. More importantly, Mattia and Le Toan [8] stated that roughness is not (truly) intrinsic, but depends on profile length, sampled distance, or measurement resolutions. They further discussed that the IEM backscattering values simulated with the local measurements of roughness show poor agreement with measured backscattering, due to the inadequate description of natural surfaces.

The other approach used for a spatial scale estimation of roughness is an inversion to extract the roughness from SAR backscattering. Lievens, et al. [12] attempted to invert effective roughness from C- and L-band SAR backscattering. From a wide range of rms height and correlation in Look Up Table (LUT), they selected optimal values to minimize retrieval errors in soil moisture and differences in backscattering with SAR measurements. A number of studies successfully applied a LUT inversion approach for the retrievals of surface roughness and soil moisture [13–16]. However, Lievens, et al. [12] stated that inverted roughness should be considered as a tuning parameter to fit with the Integral Equation Model (IEM), instead of intrinsic roughness in a geometrical sense.

Unlike the (single-scale) intrinsic roughness of a stationary process that takes into account the micro-topography (e.g., soil texture, grain size, or height variation) on the scale of radar wavelength, the fractal surface is non-stationary, and exists on multi-scales from several millimetres to meters [6,11,17,18]. 'Non-stationary' means that roughness parameters depend on the location to be measured or the profile length. However, spatial variability is periodic and self-affine. Because fractals model a common nature across the scales and self-similarity between small-scale and large-scale topography, as introduced by Mandelbrot [19], they are scale-invariant.

The backscattering from fractal surfaces is thus affected by the different ranges of roughness from stationary intrinsic surfaces. Instead of rms height, correlation length, and the ACF of roughness parameters, it is usually described by the roughness power spectrum associated with fractal dimension, spectral slopes, and other parameters. One of the most commonly used fractal models is fractional Brownian motion (fBm). With the power-law behaviour and fractal surface, researchers have made some improvements in backscattering model simulation [8,9,20]. From a variogram and power spectrum of the DEM from interferometric SAR, fractal parameters such as fractal dimension, Hurst exponent, or incremental standard deviation are retrieved and used to compare analytical

and theoretical backscattering, resulting in a good agreement [2,21]. Others attempted to re-define intrinsic roughness such as rms height and correlation length with power-law roughness spectral parameters [5,10,22]. This 'pseudo' rms height and correlation length are suggested to be profile length-dependent as non-stationary fractal roughness.

However, none of those previous studies stated above examined how fractal properties alter a partitioning of backscattering, although they emphasized the significance and sensitivity of roughness to soil moisture retrievals and investigated the influence of multi-scale roughness on backscattering simulation. Backscattering itself does not inform partitioning between soil moisture and roughness. Secondly, most of the fractal approaches stated above are based upon an empirical approach and require local information of geometric conditions. However, such information is often not available on the spatial scale. It is uncertain whether a priori knowledge will be applicable to the study area of interest. In addition, after reviewing more than a hundred publications on fractal geometry, Nayak, et al. [23] stated that fractal models may encounter errors due to the inaccuracy of fractal parameters estimated or the poor quality of an input image. In fact, SAR data are vulnerable to speckle at sub-pixel levels, and often contain calibration errors. They are not isotropic as most of fractal models assume. Thus, it is important to investigate how multi-scale roughness will affect soil moisture retrievals and backscattering partitioning.

This research aimed to answer the question of how to adopt multi-scale roughness into a radiative transfer model structure, when the isotropic assumption of the power-law spectrum is not applicable to SAR data [2,24], and to assess whether a violation of the isotropic assumption of fractal approach is more detrimental than that of a time-invariance assumption of inversion. The objectives of this study are (i) to suggest an approach to determine multi-scale roughness and (ii) to compare the effects of single-scale roughness with those of multi-scale on the IEM backscattering model and its partitioning between roughness and soil moisture. Due to a limitation of IEM, only near-bare soil conditions were considered for this study.

2. Methods

Figure 1 illustrate the Conceptual diagram for fractal approach, while Figure 2 shows the study sites.

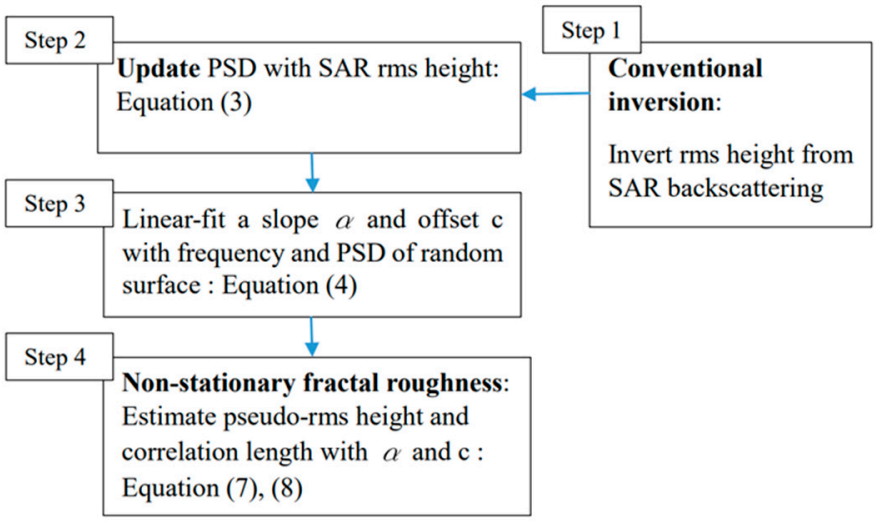

Figure 1. Conceptual diagram for fractal approach.

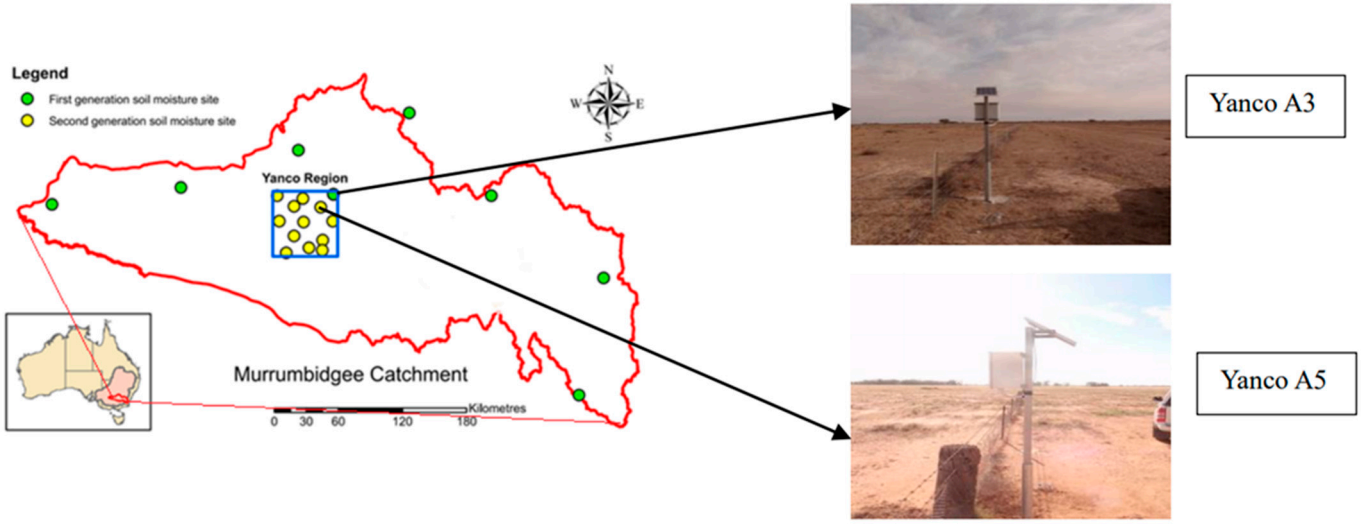

Figure 2. The Soil Moisture Monitoring Network (MSMMN, https://www.oznet.org.au, accessed on 19 August 2019) at the Murrumbidgee catchment and two Yanco sites [25].

2.1. Study Site

The Yanco site is a flat plain in southwestern New South Wales in Australia. Yanco A3 station is hereafter referred to as YA3 (latitude: 34°44′6.756″ S, longitude: 146°4′55.092″ E, elevation: 132 m). Yanco A5 is hereafter shown as YA5 (latitude: 34°42′46.2888″ S, longitude: 146°7′39.7632″ E, elevation: 136 m). The spatial domain for YA3 ranges from latitude of 34°44′23.64″ S to 34°43′55.2″ S and from longitude of 146°4′40.8″ E to 146°4′58.44″ E. YA5 ranges from latitude of 34°42′54″ S to 34°42′39.6″ S and longitude of 146°7′33.6″ E to 146°7′47.64″ E. During this study period (Day of Year (DoY) 25~145 at the YA3 site, and DoY 1~145 at the YA5 site) in 2018, the soils were near-bare with no change in vegetation growth (for example, the Leaf Area Index (LAI) was 0.2, approximately). Soil moisture measurement for these sites was obtained from the OzNet data archive (http://www.oznet.org.au/, accessed on 19 August 2019) [25]. Soil texture was silty clay (conversation with Dr. Jason Beringer). Soil temperature at the top 5 cm was 25 °C during the experimental period, approximately. Unfortunately, the measurements of surface roughness (e.g., RMS height or correlation length) and rainfall data were unavailable.

2.2. Inversion of Soil Moisture from Sentinel-1 Backscattering

Sentinel-1 operates at C-band (5.4 GHz). The 2018 data in interferometric Wide (IW) swath mode (VV + VH Polarization, descending orbit) at Ground Range Detected (GRD) were accessed on 2019-7-10 from Copernicus open access hub, processed by ESA. They have a high spatial resolution at 20 × 22 m, and a pixel spacing at 10 × 10 m. This has an improved revisit time of 12 days over the Yanco sites. Unfortunately, multi-angular data were not available over this location. The incidence angles over the study area were uniform at 35~38°, approximately. Gridded time-series SAR images were produced through pre-processing steps which included radiometric and terrain correction (Range-Doppler Terrain Correction), and multi-temporal speckle filtering. Calibration was performed by using the approach of Laur, et al. [26].

Surface roughness was inverted via IEM from SAR backscattering [27–29].

$$\sigma^{o}_{pp} = \frac{k^2}{2}\exp(-2k_z^2 s^2)\sum_{n=1}^{\infty} s^{2n}\left|I^n_{\mathrm{pp}}\right|^2 \frac{\mathrm{W}^n(-2k_{\mathrm{X}}, 0)}{n!} \quad (1)$$

where the subscript *pp* indicates the polarization, k is the wave number, and s is the rms height. In addition, $k_{\mathrm{x}} = k\sin\theta$, $k_{\mathrm{z}} = k\cos\theta$, where θ is the incidence angle. $I_{\mathrm{pp}}{}^{\mathrm{n}}$ is a function of the Fresnel reflection coefficient, relative permittivity, and permeability of the

surface, and W^n is the Fourier transform for the n th power of the normalized surface correlation function.

The IEM requires rms height, correlation length, as well as autocorrelation function at single scale for inputs [30]. To estimate these, an inversion algorithm selects the roughness values from the LUT with a wide range of rms height at 0.22~4 cm and correlation length at 0.2~11 cm when IEM simulates Sentinel-1 backscattering values [28].

$$\min \mid \sigma_{\text{sentinel-1}} - \sigma_{\text{IEM}} (\varepsilon, \text{RH}) \mid \quad (2)$$

where σ is backscattering, and the subscript describes a source of backscattering. IEM backscattering is shown as a function of the ε dielectric constant and RH soil roughness. It was assumed that roughness does not change during the acquisition of three SAR images, while soil moisture changes [12]. The roughness retrievals were further used to estimate the dielectric constants through IEM. Dielectric constant was converted to soil moisture by soil texture [31]. This is step 1 in Figure 1, where the overall procedure for estimating fractal roughness is summarized.

2.3. Fractal Roughness

In step 2 of Figure 1, we calibrate the power spectral density with SAR rms height. For a randomly rough surface where the surface height profile z(x,y) (2D surface area as A^2) follows a Gaussian random process, the statistical properties of the surface are defined by the power spectrum. The area under the power spectral density curve is equivalent to the square of rms height s [5,32], as follows:

$$S2 = \sum_{1}^{n}\sum_{1}^{m} \left| S\left(f_x, f_y\right)\right|^2 \quad (3)$$

where $S(f_x,f_y)$ is the 2D power spectral density (PSD) with spatial frequency f_x ($2\pi m/\text{A}$) and f_y ($2\pi n/\text{A}$), the number of pixels m in the x-direction, and n is the y-direction. It is estimated by fractal surface (e.g., Hurst exponent 0.5) through $f^{-2(\text{H}+1)}$ [33]. However, the PSD estimated in this way does not reflect SAR roughness characteristics as defined by IEM. PSD was thus updated and normalized using Equation (3) (e.g., multiply PSD by the ratio of s^2 from SAR and s^2 in Equation (3)). From an inverse Fast Fourier Transform of PSD, it is also possible to artificially construct the random surface with height z(x,y).

Then, in step 3 in Figure 1, from the spectral parameters obtained from random surfaces, we can estimate the non-stationary fractal roughness. The one-sided power-law spectrum is valid over the interval $0 \leq f_x \leq \infty$ [24].

$$\text{S}(f_x) = \text{c}/{f_x}^{\alpha} \quad (4)$$

where log(c) is the offset, and α is the spectral slope of the 1D profile ($1 \leq \alpha \leq 3$). By wave number $k = 2\pi f_x$, (4) can be rewritten, as follows:

$$\text{S}_\text{k}(k) = \text{C}_k/k^{\alpha} \quad (5)$$

If taking log for (4) and (5), the offsets of wave number and frequency have the following relationship [5]:

$$log(\text{c}) = log\ (\text{C}_k) - \alpha log\ (2\pi) \quad (6)$$

From linear-fitting the parameters $\text{S}_\text{k}(k)$ and k in (5) on a log-log scale as shown by Figure 3, α and c are retrieved to estimate pseudo- intrinsic roughness [5] (see Figure 3), as follows:

$$s\ (\text{L}) = \left(\frac{\text{cL}^{\alpha-1}}{\alpha-1}\right)^{\frac{1}{2}} \quad (7)$$

$$l^*(\mathrm{L}) = \frac{(\alpha-1)^2 \mathrm{L}}{2(2\alpha-1)} \tag{8}$$

where l^* is the effective correlation length, and L is the profile length. These roughness conditions were inserted to IEM. The remaining procedure to retrieve soil moisture with roughness is the same as noted in Section 2.2.

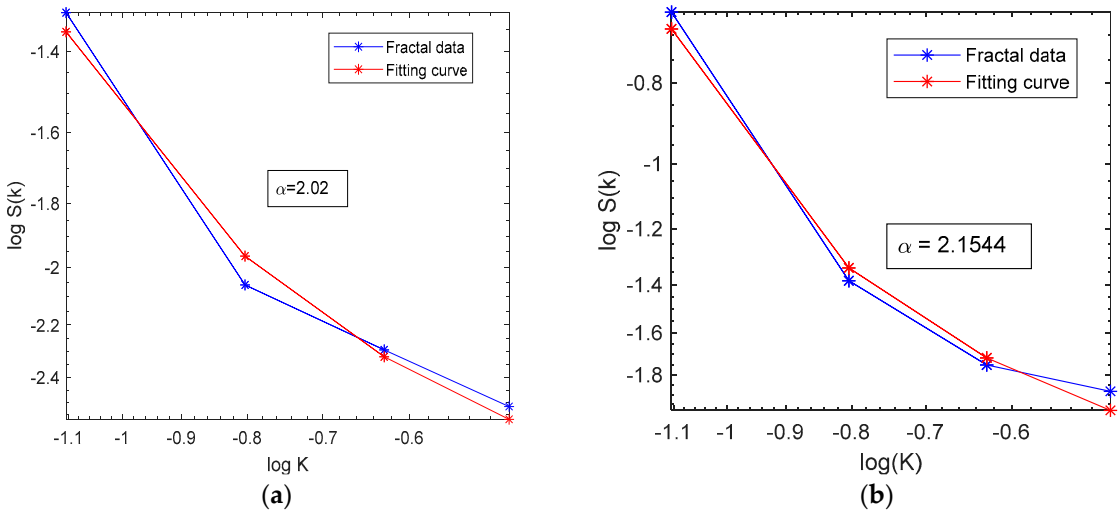

Figure 3. Fitting the slope α with log(S(k))-log(k): (**a**) Yanco 3A and (**b**) Yanco 5A.

3. Results and Discussion

The multi-scale roughness is not measurable from the intrinsic roughness locally measured in the field. Instead, we investigate the impact of multi-scale roughness on soil moisture retrievals and backscattering simulation, and discuss the difference between single- and multi-scale roughness.

3.1. Validation of Soil Moisture Retrievals at Local Point Scales

The YA3 local station is in bare soils with almost no vegetation growth. In Figure 4a,b, fractal multi-scale roughness is compared with inverted single-scale roughness. Figure 4 shows how roughness estimates change when fractals are taken into account. A quantitative comparison for local stations is illustrated in Table 1. The main difference was that inverted roughness was time-invariant due to its assumption described in Section 2.2. In contrast, fractal roughness was time-varying, although it used the same static inverted roughness as input. Additionally, the magnitudes or extents were different to each other. In other words, inversion slightly overestimated rms height and correlation length, while the fractal approach somehow underestimated them.

At the YA5 station, there is slight vegetation growth (LAI 0.2 to 0.5), suggesting a violation of the time-variance assumption used for inversion in Section 2.2. Each method suggested diverse values of roughness in Figure 5a,b, showing that the time-average of rms height is 0.22~1.47 cm, and that of correlation length is 0.57~8.63 cm. Inversion suggested more rough surfaces, but roughness decreased with increasing LAI. In contrast, the fractal approach exhibited relatively smoother surfaces and an increase with LAI, showing high correlation length at 8.63 cm. However, similarly to the YA3 station, this difference in roughness did not make much difference in the time-average of soil moisture retrievals at 0.12~0.10 m^3/m^3, RMSEs at 0.03~0.033 m^3/m^3, and cost in backscattering at 0.0126~0.0127 dB. However, a negative bias of inversion was found at -0.016 m^3/m^3 while that of the fractal approach was lower at 0.005 m^3/m^3. Because all other retrieval conditions, except roughness, were the same for both inversion and the fractal approach in YA5, this implies that IEM poorly simulated the dielectric constant with inverted roughness in roughness-varying conditions.

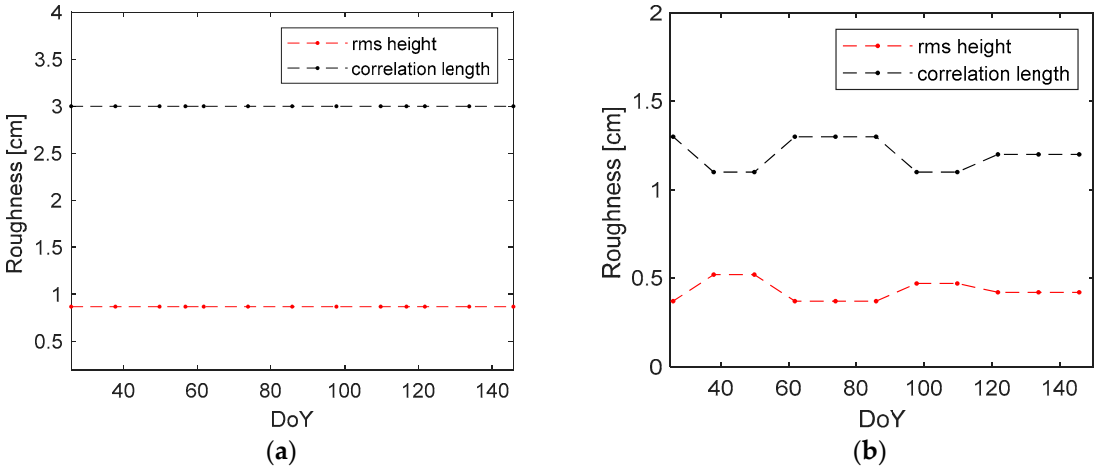

Figure 4. Temporal evolution at Yanco 3A: (**a**) inversion roughness and (**b**) fractal roughness.

Table 1. Time-average roughness and soil moisture data at local stations.

		YA3		YA5	
		Fractal	**Inversion**	**Fractal**	**Inversion**
Roughness	rms height (cm)	0.42	0.87	0.22	1.47
	Correlation length (cm)	1.22	3.00	8.63	0.57
Soil moisture	Mean (m^3/m^3)	0.04	0.037	0.12	0.10
	RMSE (m^3/m^3)	0.01	0.01	0.033	0.03
	Bias (m^3/m^3)	0.01	−0.001	0.005	−0.02
	Cost in backscattering (dB) *	0.03	0.78	0.013	0.01

* Difference is the difference between IEM and Sentinel-1 backscattering.

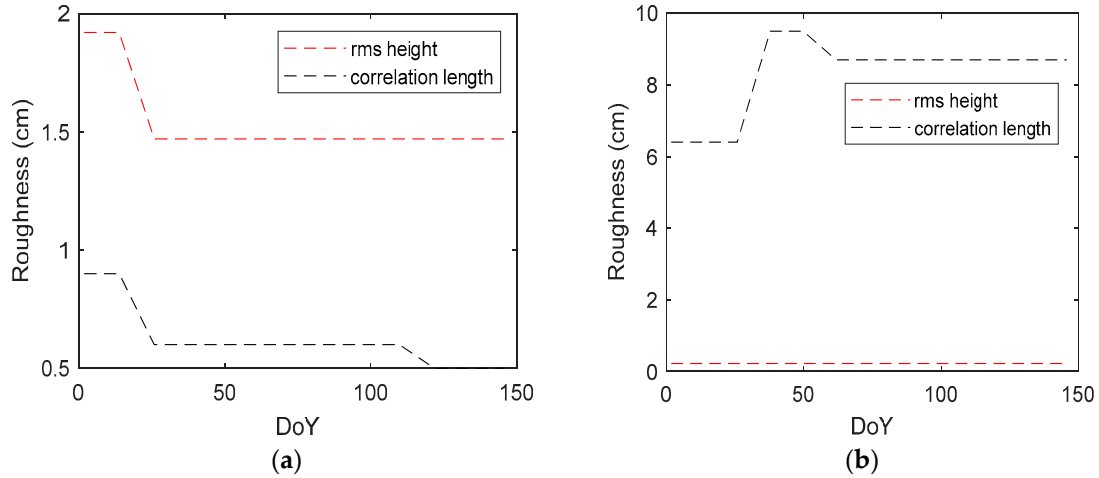

Figure 5. Temporal evolution at Yanco 5A: (**a**) inversion roughness and (**b**) fractal roughness.

However, these dissimilar values of roughness did not make much difference in soil moisture retrieval outputs, as shown in Figure 6a. More specifically, in Table 1, the soil moisture RMSE of inversion was 0.01 m^3/m^3, while that of the fractal approach was

0.012 m^3/m^3. Their time-average of consequent soil moisture retrievals was similar at 0.037~0.044 m^3/m^3, although rms height was varied at 0.4~0.9 cm, and correlation length was varied at 1.2~3 cm. Given that all other retrieval conditions, except roughness, were set to be the same for both inversion and fractal approach, this convergence is considered because of the equa-finality of a radiative transfer model, meaning that different composites of dielectric constant and surface roughness produce the same backscattering coefficient [11]. However, it is stated that the performance of IEM was different. In Table 1, when a cost in backscattering ($\Delta\sigma^{\circ}$) of inversion is higher at 0.78 dB, there was almost no bias at -0.000905 m^3/m^3. This implies that IEM poorly simulated backscattering with inverted roughness. For comparison, the difference in backscattering was 0.03 dB for fractal roughness.

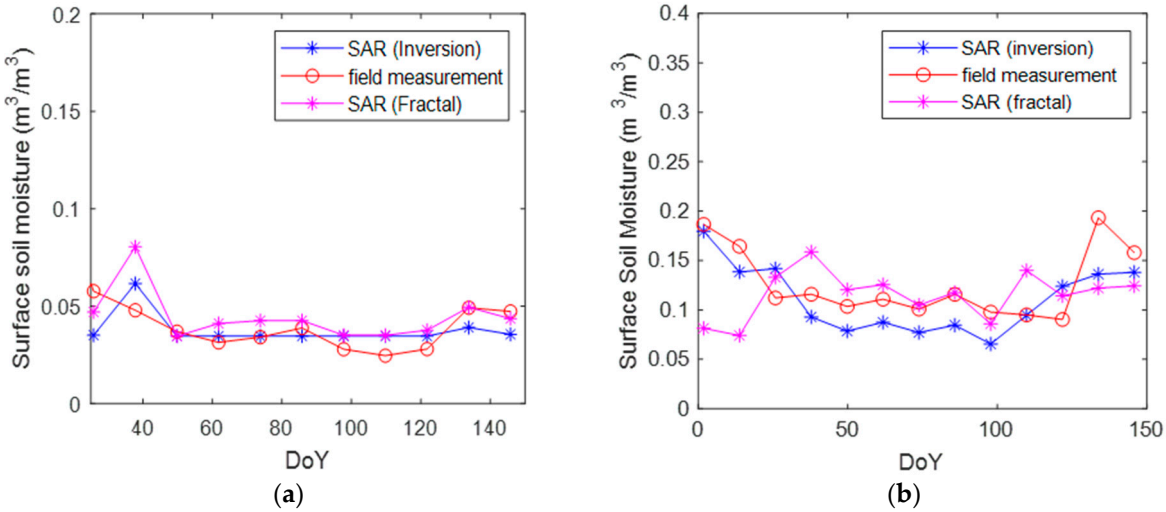

Figure 6. Time-series surface soil moisture: (**a**) YA3 and (**b**) YA5.

Taken together, in this Yanco site, fractal roughness is likely to better represent geometrical properties, because fractal roughness better reduced a retrieval bias in roughness-varying YA5 and simulated backscattering at YA3 at an acceptable bias level. This is considered because the time-invariance assumption of inversion was violated. In natural surfaces, roughness often changes, because soil evaporates, rain falls, and vegetation changes.

This statement is also valid in consideration of a priori knowledge. More specifically, the time-average of inverted correlation length at YA5 was found to be extremely low at 0.57 cm, given the rough surface with rms height of 1.47 cm. This level of correlation length was also out of a normal range (2~20 cm) of intrinsic correlation length often found over various surfaces [9,10]. In contrast, fractal roughness was within a geometrically typical range of the intrinsic roughness values normally suggested for both rms height and correlation length, although fractal roughness does not necessarily need to be in accordance with single-scale intrinsic roughness.

3.2. Spatial Distribution of Surface Roughness: Single-Scale vs. Multi-Scale

In Figure 7, the YA3 site was found to be anisotropic. The inverted rms height is spatially compared with the fractal approach which can be violated by the isotropic assumption. The spatial average of inversion was slightly higher at 0.982 cm than that of fractal approach at 0.574 cm. So was the spatial variation. However, the overall spatial distribution patterns themselves were similar to each other, implying that a fractal estimation seems to be influenced by inverted rms height as input. Similarly, in the less anisotropic YA5 in Figure 8, the spatial average of inversion was slightly higher at 0.78 cm than that of the fractal approach at 0.23 cm. Taken together, the fractal approach suggested smoother surfaces at both sites, and its pattern was similar to that of inversion.

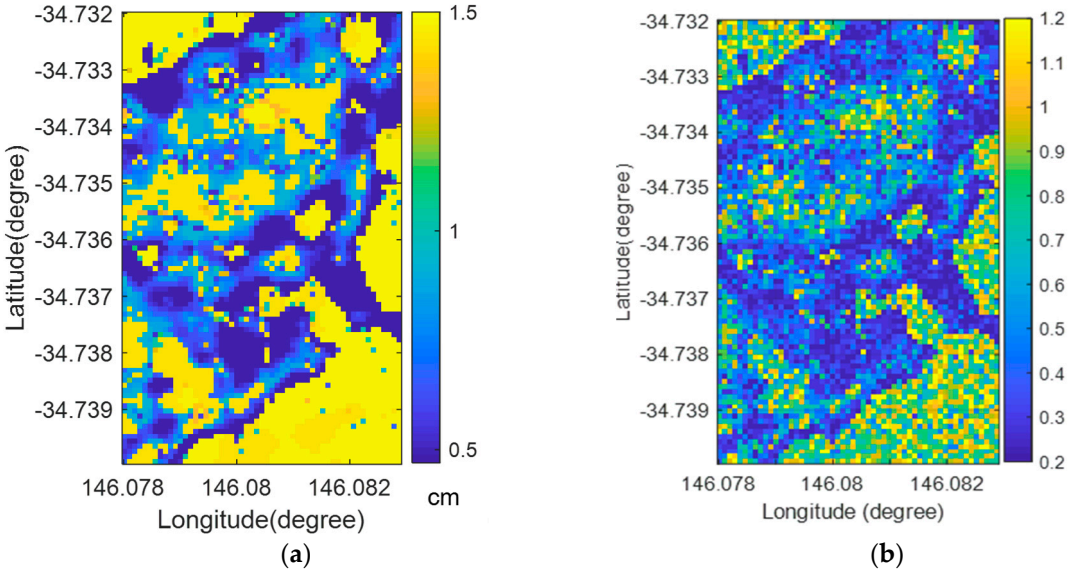

Figure 7. Spatial distribution of rms height at YA3 on DoY 49: (**a**) inversion and (**b**) fractal approach.

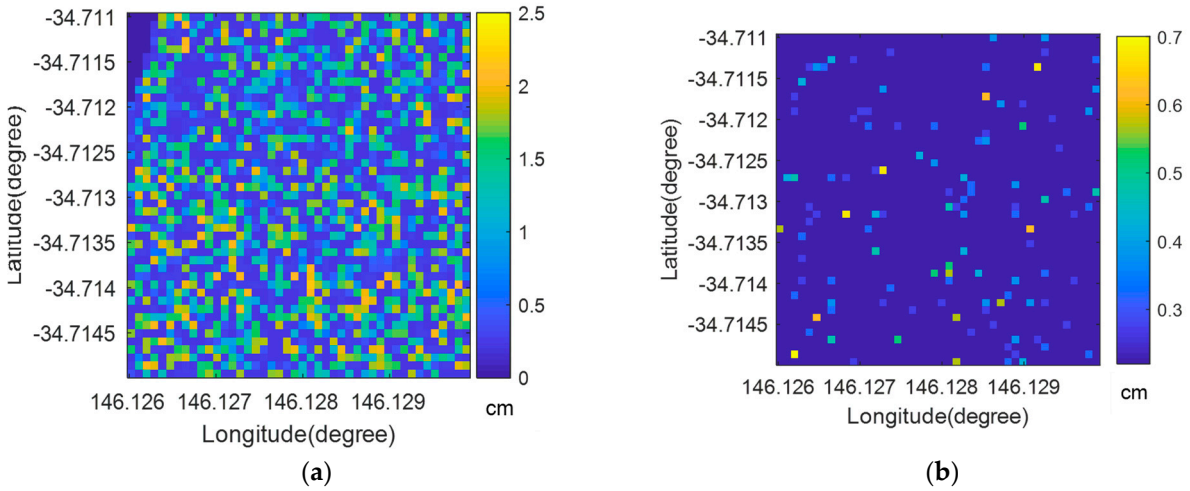

Figure 8. Spatial distribution of rms height at YA5 on DoY 73: (**a**) inversion and (**b**) fractal approach.

However, when it comes to correlation length, their spatial patterns contrasted with each other. In Figure 9, the inverted correlation length at the YA3 site is compared with the fractal approach. Similarly to the single-scale rms height, the spatial average of the inverted correlation length was higher at 4.1 cm than that of the fractal approach at 1.47 cm. The areas with a higher correlation length (shown in yellow in Figure 9a) in inversion were suggested to have lower levels (shown in green and blue in Figure 9b) in the fractal approach. In other words, the spatial distribution of the inverted correlation length had a negative relationship with that of rms height (i.e., smooth areas with lower rms height have a higher correlation length). In contrast, the fractal approach had a positive relationship for the spatial distribution of roughness (i.e., rough areas with higher rms height also have a higher correlation length) [33]. At the less anisotropic YA5 site, roughness was spatially random, less likely violating the assumption of fractal models. In Figure 10, the spatial average of the inverted correlation length was lower at 3.18 cm than that of the fractal approach at 9.42 cm.

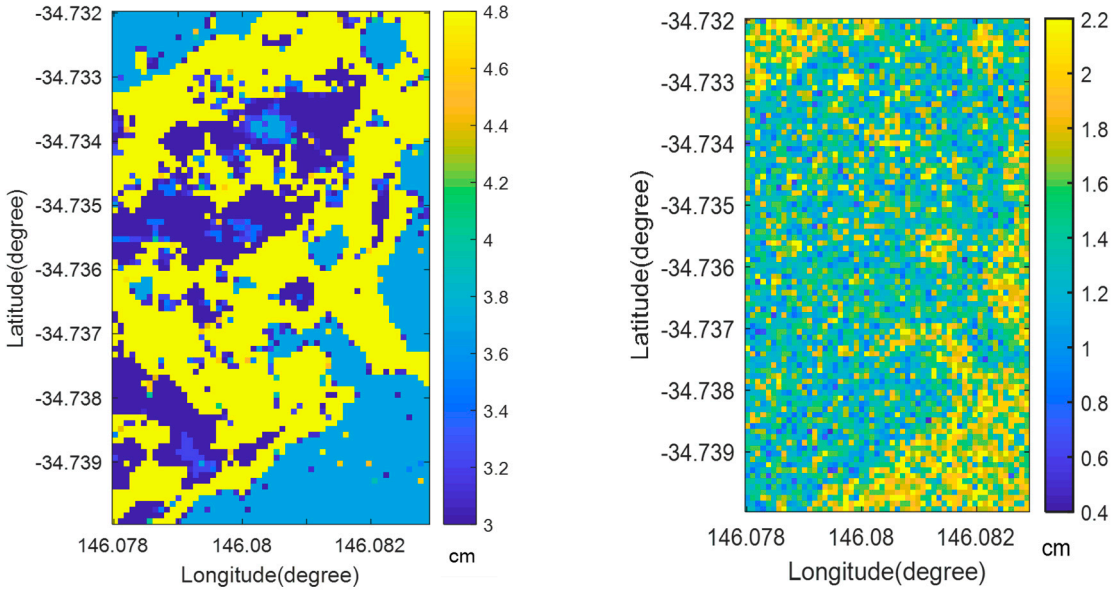

Figure 9. Spatial distribution of correlation length at YA3 on DoY 49: (**a**) inversion and (**b**) fractal approach.

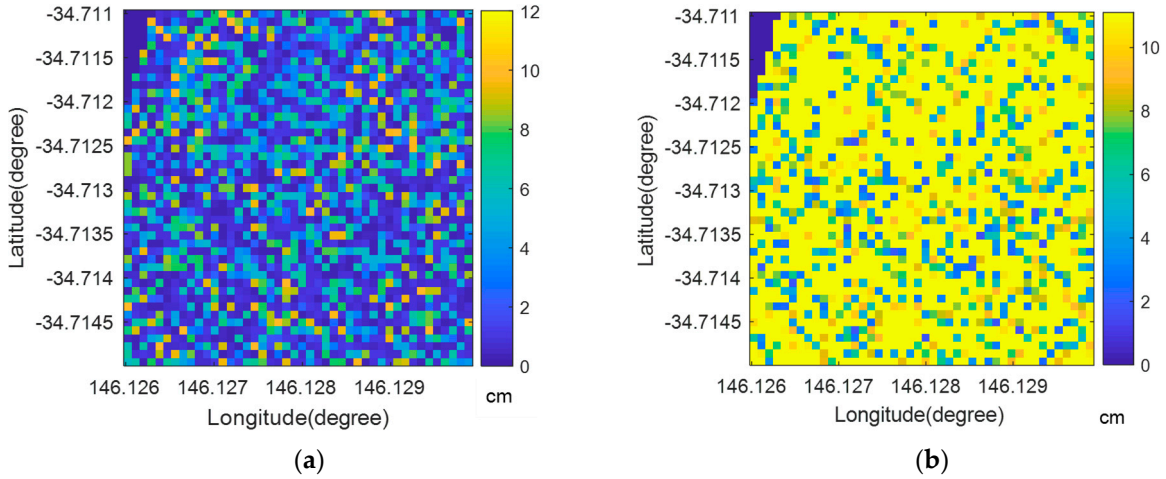

Figure 10. Spatial distribution of correlation length at YA5 on DoY 73: (**a**) inversion and (**b**) fractal approach.

3.3. Impact of Roughness on Surface Soil Moisture Retrievals

Figure 11 shows the spatial distribution of soil moisture retrievals and related variables at the anisotropic YA3 site. As illustrated by local validation in Figure 6a, both inversion and the fractal approach agree with the fact that it is mostly very dry. The spatially averaged soil moisture of inversion was found to be 0.052 m^3/m^3, while that of the fractal approach was 0.061 m^3/m^3. With respect to the elevated backscattering shown in yellow in Figure 11c, both methods agree with the fact that roughness contributed to backscattering more than soil moisture. In more detail, inversion showed a strong relationship between backscattering and correlation length, while fractal roughness exhibited a contribution marginally from soil moisture and partially from rms height. Interestingly, although the isotropic assumption was violated at this site, the cost minimization of backscattering for the fractal approach was smaller at 0.42 dB as the spatial average, compared to that of inversion at 0.878 dB. This suggests that this approach may mitigate the effects from the assumption violation of the fractal model.

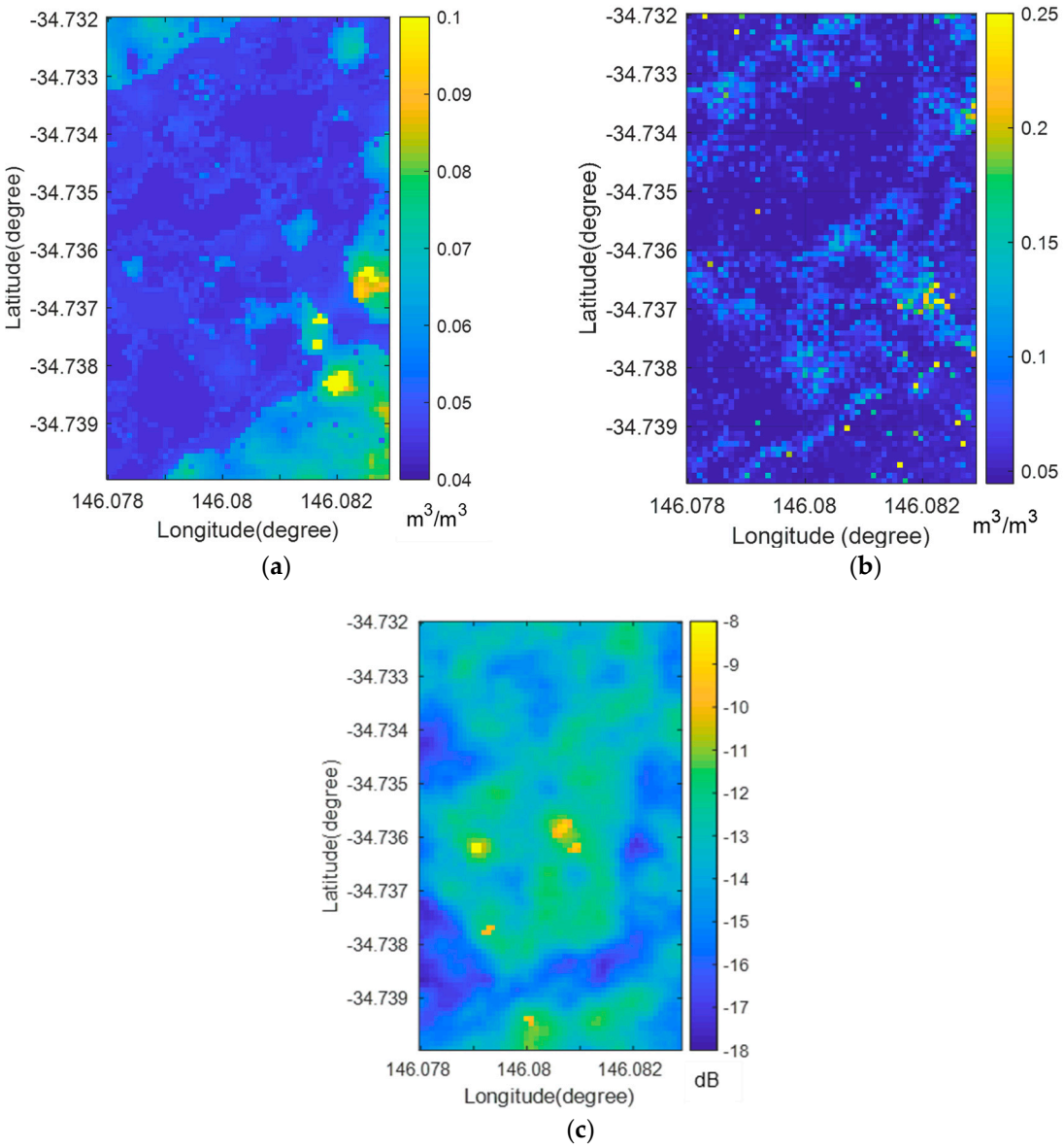

Figure 11. Spatial distribution around YA3 site on DoY 49: (**a**) surface soil moisture (m^3/m^3) estimated using inversion; (**b**) surface soil moisture (m^3/m^3) estimated using the fractal approach; and (**c**) Sentinel-1 backscattering.

Figure 12 shows that fractal roughness better captured the strong contribution of soil moisture to backscattering at the less anisotropic and wetter YA5 site. Similarly to local validation in Figure 6b, both inversion and the fractal approach agree with the fact that it is moderately wet. The spatial average of inverted soil moisture was found to be 0.11 m^3/m^3, while that of the fractal approach was 0.18 m^3/m^3. However, there was disagreement over the area shown in green in Figure 12b. Over this area, the fractal approach reported wetter soils than inversion. Considering that this wetter area shows higher backscattering, shown in yellow in Figure 12c (the spatial average of Sentine-1 backscattering: −17.1 dB) but there is no particular increase in roughness, the fractal approach clearly suggests that soil moisture is a main contributor to backscattering over this area. In contrast, such a feature is less clear in inversion. The fact that the soil moisture distribution of the fractal approach is coincident with that of the backscattering measurement satisfies the theoretical relationship between the dielectric constant and backscattering. Combining this positive spatial relationship with a local validation of fractal roughness that showed a reduced bias at YA5 in Section 3.1 and Table 1, it is suggested that the use of multi-scale roughness may

be able to overcome the limitation of inversion arising from the time-invariance assumption (there was a slight change in vegetation from LAI of 0.2 to 0.5). The cost in backscattering of the fractal approach was higher at 0.25 dB on spatial average, as compared to inversion at 0.0154 dB. However, as compared to the anisotropic YA3 site at 0.4~0.9 dB, this value is lower and acceptable.

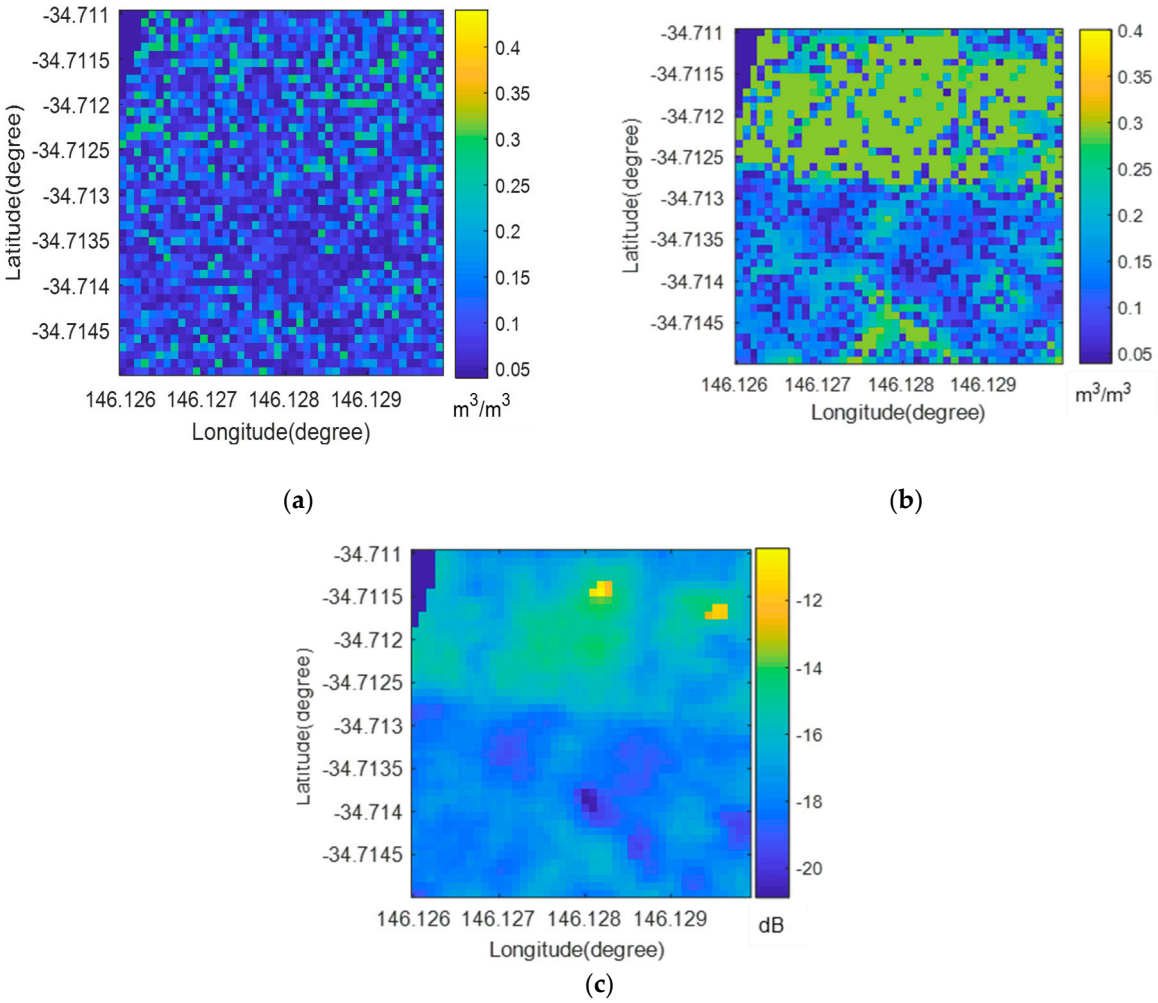

Figure 12. Spatial distribution around the YA5 site on DoY 73: (**a**) surface soil moisture (m^3/m^3) estimated using inversion; (**b**) surface soil moisture (m^3/m^3) estimated using the fractal approach; and (**c**) Sentinel-1 backscattering.

4. Conclusions

A novel method to estimate spectral parameters from SAR-retrieved rms height was proposed. It was investigated whether fractal roughness can better simulate IEM than inversion. Both have different limitations. Inversion is restricted by the time-invariance assumption of roughness, while it is assumed to be isotropic for the fractal model.

In anisotropic bare soils, local validation shows that IEM poorly simulated backscattering with inverted single-scale roughness. In the isotropic soils at YA5, fractal roughness better reduced retrieval biases. From the spatial comparison of soil moisture and roughness, we found that the fractal approach seems to better represent a partitioning of Sentinel-1 backscattering. In the dry conditions at YA3, both methods reported that roughness contributed more to the elevation of backscattering. Although the isotropic assumption was violated, IEM better converged to Sentine-1 backscattering using the fractal model. In the less anisotropic but wetter YA5, the fractal approach clearly showed a positive relationship between Sentinel-1 backscattering and soil moisture.

It is thus suggested that a multi-scale fractal approach better simulated IEM and hydrological features, regardless of isotropic orientation. However, there is a limitation in this approach. Due to fundamental limitations of IEM, only near-bare soil with no dense vegetation was investigated. To further develop this approach, future work will extend this suggested method to larger study domains with volume scattering of vegetation.

Author Contributions: Conceptualization, J.H.L.; methodology, J.H.L.; software, J.H.L.; validation, J.H.L.; formal analysis, J.H.L.; investigation, J.H.L.; resources, J.H.L.; data curation, J.H.L.; writing—original draft preparation J.H.L.; writing—review and editing, J.H.L. and H.-C.K.; visualization, J.H.L.; supervision, J.H.L.; project administration, J.H.L.; funding acquisition, J.H.L. All authors have read and agreed to the published version of the manuscript.

Funding: This research was funded by Global Water Futures program.

Data Availability Statement: We can share data, upon request.

Conflicts of Interest: The authors declare no conflicts of interest.

References

1. Abdelsalam, M.G.; Stern, R.J. Mapping Precambrian structures in the Sahara Desert with SIR-C/X-SAR radar: The Neoproterozoic Keraf Suture, NE Sudan. *J. Geophys. Res. Planets* **1996**, *101*, 23063–23076. [CrossRef]
2. Di Martino, G.; Riccio, D.; Zinno, I. SAR Imaging of Fractal Surfaces. *IEEE Trans. Geosci. Remote Sens.* **2012**, *50*, 630–644. [CrossRef]
3. Voigt, S.; Kemper, T.; Riedlinger, T.; Kiefl, R.; Scholte, K.; Mehl, H. Satellite Image Analysis for Disaster and Crisis-Management Support. *IEEE Trans. Geosci. Remote Sens.* **2007**, *45*, 1520–1528. [CrossRef]
4. Evans, D.L.; Farr, T.G.; Zyl, J.J.v. Estimates of surface roughness derived from synthetic aperture radar (SAR) data. *IEEE Trans. Geosci. Remote Sens.* **1992**, *30*, 382–389. [CrossRef]
5. Dierking, W. Quantitative roughness characterization of geological surfaces and implications for radar signature analysis. *IEEE Trans. Geosci. Remote Sens.* **1999**, *37*, 2397–2412. [CrossRef]
6. Weeks, R.; Smith, M.; Pak, K.; Gillespie, A. Inversions of SIR-C and AIRSAR data for the roughness of geological surfaces. *Remote Sens. Environ.* **1997**, *59*, 383–396. [CrossRef]
7. Gorrab, A.; Zribi, M.; Baghdadi, N.; Mougenot, B.; Fanise, P.; Chabaane, Z.L. Retrieval of Both Soil Moisture and Texture Using TerraSAR-X Images. *Remote Sens.* **2015**, *7*, 10098–10116. [CrossRef]
8. Mattia, F.; Le Toan, T. Backscattering Properties of Multi-Scale Rough Surfaces. *J. Electromagn. Waves Appl.* **1999**, *13*, 493–527. [CrossRef]
9. Zribi, M.; Ciarletti, V.; Taconet, O. Validation of a Rough Surface Model Based on Fractional Brownian Geometry with SIRC and ERASME Radar Data over Orgeval. *Remote Sens. Environ.* **2000**, *73*, 65–72. [CrossRef]
10. Maleki, M.; Amini, J.; Notarnicola, C. Soil roughness retrieval from TerraSar-X data using neural network and fractal method. *Adv. Space Res.* **2019**, *64*, 1117–1129. [CrossRef]
11. Kornelsen, K.; Coulibaly, P. Advances in soil moisture retrieval from synthetic aperture radar and hydrological applications. *J. Hydrol.* **2013**, *476*, 460–489. [CrossRef]
12. Lievens, H.; Verhoest, N.E.C.; De Keyser, E.; Vernieuwe, H.; Matgen, P.; Álvarez-Mozos, J.; De Baets, B. Effective roughness modelling as a tool for soil moisture retrieval from C- and L-band SAR. *Hydrol. Earth Syst. Sci.* **2011**, *15*, 151–162. [CrossRef]
13. Merzouki, A.; McNairn, H.; Pacheco, A. Mapping Soil Moisture Using RADARSAT-2 Data and Local Autocorrelation Statistics. *IEEE J. Sel. Top. Appl. Earth Obs. Remote Sens.* **2011**, *4*, 128–137. [CrossRef]
14. Rabus, B.; Wehn, H.; Nolan, M. The Importance of Soil Moisture and Soil Structure for InSAR Phase and Backscatter, as Determined by FDTD Modeling. *IEEE Trans. Geosci. Remote Sens.* **2010**, *48*, 2421–2429. [CrossRef]
15. Rahman, M.M.; Moran, M.S.; Thoma, D.P.; Bryant, R.; Holifield Collins, C.D.; Jackson, T.; Orr, B.J.; Tischler, M. Mapping surface roughness and soil moisture using multi-angle radar imagery without ancillary data. *Remote Sens. Environ.* **2008**, *112*, 391–402. [CrossRef]
16. Rahman, M.M.; Moran, M.S.; Thoma, D.P.; Bryant, R.; Sano, E.E.; Holifield Collins, C.D.; Skirvin, S.; Kershner, C.; Orr, B.J. A derivation of roughness correlation length for parameterizing radar backscatter models. *Int. J. Remote Sens.* **2007**, *28*, 3995–4012. [CrossRef]
17. Davidson, M.W.J.; Thuy Le, T.; Mattia, F.; Satalino, G.; Manninen, T.; Borgeaud, M. On the characterization of agricultural soil roughness for radar remote sensing studies. *IEEE Trans. Geosci. Remote Sens.* **2000**, *38*, 630–640. [CrossRef]
18. Mattia, F.; Davidson, M.W.J.; Toan, T.L.; Haese, C.M.F.D.; Verhoest, N.E.C.; Gatti, A.M.; Borgeaud, M. A comparison between soil roughness statistics used in surface scattering models derived from mechanical and laser profilers. *IEEE Trans. Geosci. Remote Sens.* **2003**, *41*, 1659–1671. [CrossRef]
19. Mandelbrot, B.B. *The Fractal Geometry of Nature*, Revised and Enlarged ed.; WH Freeman: New York, NY, USA, 1983.
20. Franceschetti, G.; Iodice, A.; Migliaccio, M.; Riccio, D. Scattering from natural rough surfaces modeled by fractional Brownian motion two-dimensional processes. *IEEE Trans. Antennas Propag.* **1999**, *47*, 1405–1415. [CrossRef]

21. Martino, G.D.; Iodice, A.; Riccio, D.; Ruello, G. A Novel Approach for Disaster Monitoring: Fractal Models and Tools. *IEEE Trans. Geosci. Remote Sens.* **2007**, *45*, 1559–1570. [CrossRef]
22. Ghafouri, A.; Amini, J.; Dehmollaian, M.; Kavoosi, M.A. Better Estimated IEM Input Parameters Using Random Fractal Geometry Applied on Multi-Frequency SAR Data. *Remote Sens.* **2017**, *9*, 445. [CrossRef]
23. Nayak, S.R.; Mishra, J.; Palai, G. Analysing roughness of surface through fractal dimension: A review. *Image Vis. Comput.* **2019**, *89*, 21–34. [CrossRef]
24. Di Martino, G.; Iodice, A.; Riccio, D.; Ruello, G. Imaging of Fractal Profiles. *IEEE Trans. Geosci. Remote Sens.* **2010**, *48*, 3280–3289. [CrossRef]
25. Smith, A.B.; Walker, J.P.; Western, A.W.; Young, R.I.; Ellett, K.M.; Pipunic, R.C.; Grayson, R.B.; Siriwardena, L.; Chiew, F.H.S.; Richter, H. The Murrumbidgee soil moisture monitoring network data set. *Water Resour. Res.* **2012**, *48*, W07701. [CrossRef]
26. Laur, H.; Bally, P.; Meadows, P.; Sanchez, J.; Schaettler, B.; Lopinto, E.; Esteban, D. ERS SAR calibration. Derivation of the backscattering coefficient in ESA ERS SAR PRI products. *ESA/ESRIN ES-TN-RS-PM-HL09* **2004**, *2*. Available online: https://earth.esa.int/eogateway/documents/20142/37627/ERS-SAR-Calibration-Issue2.f_05_DLFE-643.pdf (accessed on 9 October 2023).
27. van der Velde, R.; Su, Z.; van Oevelen, P.; Wen, J.; Ma, Y.; Salama, M.S. Soil moisture mapping over the central part of the Tibetan Plateau using a series of ASAR WS images. *Remote Sens. Environ.* **2012**, *120*, 175–187. [CrossRef]
28. Lee, J.H.; Walker, J. Inversion of soil roughness for estimating soil moisture from time-series Sentinel-1 backscatter observations over Yanco sites. *Geocarto Int.* **2020**, *37*, 1850–1862. [CrossRef]
29. Lee, J.H.; Lindenschmidt, K.-E. Bias-Corrected RADARSAT-2 Soil Moisture Dynamics Reveal Discharge Hysteresis at An Agricultural Watershed. *Remote Sens.* **2023**, *15*, 2677. [CrossRef]
30. Fung, A.K. *Microwave Scattering and Emission Models and Their Applications*; Artech House: Norwood, MA, USA, 1994.
31. Reynolds, C.A.; Jackson, T.J.; Rawls, W.J. Estimating soil water-holding capacities by linking the Food and Agriculture Organization Soil map of the world with global pedon databases and continuous pedotransfer functions. *Water Resour. Res.* **2000**, *36*, 3653–3662. [CrossRef]
32. Mahboob Kanafi, M.; Tuononen, A.J. Top topography surface roughness power spectrum for pavement friction evaluation. *Tribol. Int.* **2017**, *107*, 240–249. [CrossRef]
33. Persson, B.N.J.; Albohr, O.; Tartaglino, U.; Volokitin, A.I.; Tosatti, E. On the nature of surface roughness with application to contact mechanics, sealing, rubber friction and adhesion. *J. Phys. Condens. Matter* **2005**, *17*, R1. [CrossRef] [PubMed]